Recent advances on solar water splitting using hematite nanorod film produced by purpose-built material methods

Waldemir Moura de Carvalho Jr. and Flavio Leandro Souza[a)]
Centro de Ciências Naturais e Humanas, Universidade Federal do ABC, Santo André, São Paulo 09210-170, Brazil

(Received 20 May 2013; accepted 24 September 2013)

Photoelectrochemical cells offer a more elegant, clean, and sustainable way to store solar energy as chemical energy through the splitting of water into its primitive form (H_2 and O_2). Among many metal oxides pointed as candidates for this application, the fundamental characteristics of hematite (α-Fe_2O_3), such as abundance, excellent chemical stability in an aqueous environment, and favorable optical band gap, emerged as a promising photoanode. Although attractive, the poor optoelectronic properties necessitate a large application of overpotential for split water assisted by solar irradiation, limiting the high performance of this material. Since the electrode was built using materials in nanoscale, significant advances were achieved. This review highlights new insights and recent progress in the use of a purpose-built material process to build hematite electrodes for improving photocatalytic activity. In addition, reduction on the required overpotential by effective control-treatment of morphology and surface of vertically aligned hematite nanorods will be addressed. An interesting set of results were also discussed revisiting a novel strategy recently presented in the literature and complementary advances was illustrated. These latest efforts aid in pointing out the challenges or obstacles to be overcome using this morphology and in defining new opportunities.

I. INTRODUCTION

Nowadays, the storage and conversion of energy into chemical fuels from sunlight by water oxidation has become one of the most exciting topics in the energy field. Water and sunlight playing in harmony can provide a clean, unlimited, sustainable, and renewable energy free from carbon produced by photoelectrochemical (PEC) water splitting using a photosensible material. Fujishima and Honda[1] were pioneers in demonstrating the photocatalytic effect using a semiconductor material to directly convert sunlight irradiation into chemical energy (hydrogen and oxygen). Since this seminal work, the PEC cell has been considered a more elegant and practical way to produce environmentally friendly fuels.[2–5] For this purpose, many semiconductor materials such as WO_3[6–10]or TiO_2[11,12] were exploited as photoanodes in PEC cells exhibiting considerable activity; however, due to their low stability in aqueous ambient and/or large band gap conferred a low usable portion of the solar spectrum, limiting commercial utilization.[4,13–15] In the last decade, experimental and theoretical studies have been dedicated to finding an ideal material to efficiently mimic nature by artificially producing the biologic photosynthesis.[10,12,16–22] In this context, hematite arise as the cheapest and most promising semiconductor material due to its natural abundance, low band gap (2.1 eV, allowing absorption of a large portion of solar irradiation), high stability in an aqueous environment, favorable valence band edge for photo-water-oxidation, and up to 12.9% efficiency predicted theoretically.[4,23] Although hematite meets many requirements, the efficiency reported until now is far from the theoretical prediction. For instance, as a consequence of hematite light absorption, the paths of photogenerated electron–hole pairs occur by promotion of electrons from valence to the conduction band and the electron vacancies (holes) from valence band to surfaces for oxidizing water. The electron vacancies (holes) have a short diffusion length of around 2–4 nm,[24–26] which means that the electron vacancy is generally filled by electrons before reaching the surface, drastically increasing the recombination rate.[27] The origin of the electronic states of these electrons is poorly understood. Moreover, the poor electronic conductivity ($\sim 10^{-2}$ $cm^2/V/s$) can be also responsible for inefficient photoanode performance. Hematite electronic conductivity has been recently reviewed, and after decades of investigation, the electronic transport of this semiconductor remains not completely understood.[4,28–32]

To overcome these limitations, many efforts have been focused on the development of different nanostructures[33–38] modifying the hematite surface by doping,[36,39–45] prelayer deposition of metal oxide[46,47] and an undoped ultrathin layer mainly for combining light penetration depths with hole length diffusion and electron collection to increase hematite efficiency.[14,48–50]

a)Address all correspondence to this author.
e-mail: fleandro.ufabc@gmail.com, flavio.souza@pq.cnpq.br
DOI: 10.1557/jmr.2013.302

 © Materials Research Society 2013

https://doi.org/10.1557/jmr.2013.302 Published online by Cambridge University Press

The first results showing the relevance of building hematite films with morphology in nanoscale were reported by Grätzel et al.[15,51] This strategy of using nanostructured films has been considered an unique solution in PEC cell applications. Since that time, several synthetic routes have been reported to produce nanostructured hematite with a variety of morphology,[52] some of which include sol–gel,[48,53,54] anodic aluminum oxide (AAO),[55] sonoeletrochemical anodization,[56] spray pyrolysis,[57] ultrasonic spray pyrolysis,[58] atmospheric pressure chemical vapor deposition (APCVD),[4,40,59] vapor phase deposition,[56,60,61] thermal pyrolysis,[57,62] atomic layer deposition (ALD),[63,64] colloidal dispersion of nanocrystal,[65] eletrodeposition,[66,67] solvothermal,[68–70] and hydrothermal processes.[71–74] From this variety of synthetic routes, the most promising nanostructures developed show a remarkable photocurrent allied to low overpotential reported in the last five years are related to APCVD, ALD, colloidal nanocrystal, and the hydrothermal method. Figure 1 illustrates some examples of successful morphologies synthesized by APCVD and colloidal nanocrystal route that provides great PEC performance.

The pure hematite films prepared from the colloidal nanocrystal approach [Figs. 1(a) and 1(b)] show a high photocurrent around 1.1 mA/cm^2 at 1.23 V_{RHE} with an onset potential as low as 0.8 V_{RHE} (under backside illumination in AM 1.5G sunlight of 1000 W/m^2). The PEC performance can be comparable to the best hematite modified with different catalysts.[35] The hematite cauliflower films doped with different catalysts such as SiO_2 or IrO_2 grown by the APCVD method [Fig. 1(c)] on the fluorine-doped tin oxide (FTO) conductor glass substrate showed a higher photocurrent from 2.2 to 3.0 mA/cm^2 at 1.23 V_{RHE} in AM 1.5G sunlight of 1000 W/m^2.[40,41] These photocurrent values starting at a low onset potential remain unmatched for any other oxide. Recently, these nanostructures were the focus of an interesting discussion in the literature, which the authors point out these morphologies as champion nanostructures for solar water splitting. They correlate

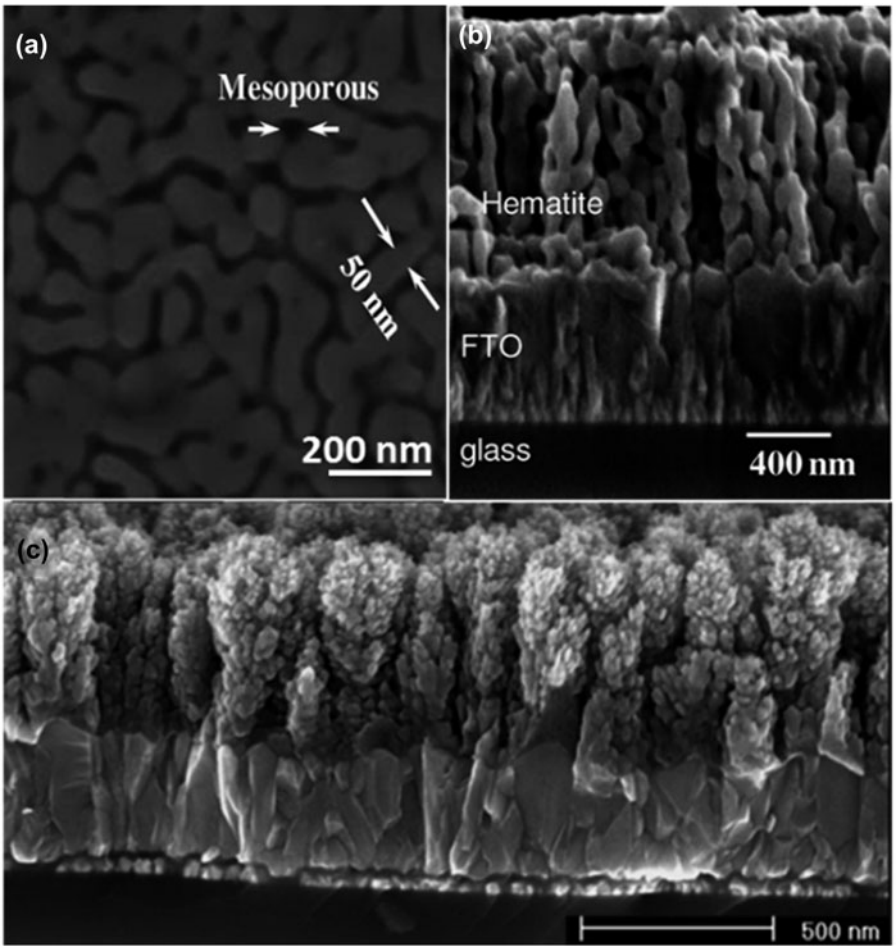


FIG. 1. SEM images of hematite nanostructures: (a) top-view and (b) cross section of six layers of mesoporous hematite films prepared by colloidal dispersion magnetite nanocrystals approach, and (c) top view of nanocauliflower hematite developed by APCVD method. Reprinted with permission from Refs. 35 and 40. Copyright 2006 and 2011, American Chemical Society.

https://doi.org/10.1557/jmr.2013.302 Published online by Cambridge University Press

the morphology with an efficient charge transport for explaining the remarkable performance.[75]

Alternatively to these nanostructures, a one-dimensional structure such as nanowire or nanorod vertically aligned, FTO conductor glass substrate has been pointed out as an optimal architecture for PEC water splitting. The reasons are large surface area and short diffusion length perpendicular to the charge-collecting substrate leading to lower recombination. For instance, hematite films composed by vertically aligned nanorods on the FTO conductor glass substrate could satisfy two important requirements; a high absorption coefficient (absorbing significant fraction of solar spectrum) and a wire/rod diameter (between 5 and 20 nm) close to the charge carrier diffusion length.[28,30] It is well known that, the band gap determines the region of the light or solar spectra the material is able to absorb. However, the fractions, f, of the photons that will be really absorbed by the materials are dependent on the absorption coefficient, α, and thickness, l, as summarized in the Beer's Law by the equation below:

$$f = 1 - e^{-\alpha l} \quad . \tag{1}$$

As previously reported, for hematite to reach 95% of light absorption at 550 nm, the films must be 0.4-μm thick, a requirement easily achieved for films composed of nanowires or nanorods without compromising their diameter size.[14]

Another requirement satisfied by films composed of one-dimensional nanostructures vertically aligned on the substrates is the morphology favorable to the electron–hole diffusion because the light absorption can be decoupled from the charge carrier diffusion length. This means that the photogenerated carriers must only reach the rod surface before recombination, contrary to films composed of nanoparticles or planar morphology wherein the carriers must travel the entire thickness of the electrode to be collected, increasing the recombination possibility. This distance that the carrier must diffuse before recombination is called diffusion length, L_D, and described as following in the equation below:

$$L_D = \sqrt{D\tau} \quad , \tag{2}$$

where D is the minority carrier diffusion coefficient, and τ is the minority carrier lifetime. Particularly for hematite with vertical rod morphology to achieve the highest performance, the radius must be similar to L_D, i.e., the available area needs to be large enough to allow collecting all the carriers. More details about the carrier diffusion length on nanostructured materials can be found in a recent review.[28]

Hematite films with morphology composed by vertically aligned nanorods, nanotubes, or nanowires can be obtaining by different methods such as metal organic vapor deposition,[76] electrochemical deposition using AAO templates,[55,77] thermal oxidation and pyrolysis,[78–80] ALD,[81] APCVD,[40] hydrothermal and solvothermal processes.[71–73,82–84] The hydrothermal approach has been extensively studied offering a simple experimental apparatus, easy control of rod or wire size, and large scale production. Among different strategies for building metal oxide nanostructured films in hydrothermal conditions, the purpose built material (PBM) process has recently gained special attention (for the past two decades since its first report).[85]

In this context, we address the current status and recent progress in improvements reached on photocatalytic performance using vertically aligned hematite nanorod photoanodes with respect to aqueous systems under hydrothermal conditions (called PBM). Several research groups in the world have been dedicated great efforts to contribute to the understanding of the fundamental properties of hematite nanorods synthesized by the PBM process (such as the work done by Mao et al.[86–88]) but will not be discussed in this manuscript.

II. HYDROTHERMAL

A. PBM method

The hydrothermal approach has attracted scientists and those from the industrial sector along the years because this process offers a low effective cost and easy production on a large scale. The term hydrothermal has a purely geological origin and can be defined as any heterogeneous reaction in the presence of an aqueous solvent or mineralizers under pressure and temperature.[89] More details about the origin and definition of the term hydrothermal are reviewed by Byrappa and Yoshimura[89] in their Handbook. The action of water at an elevated temperature and pressure was first observed in the earth's crust as it leads to the formation of rocks and minerals by the British geologist Sir Roderick Murchison. From this observation, the hydrothermal approach was probably developed and adopted by Schafthaul to produce quartz crystals.[89] Since that time, the hydrothermal technique became a very useful route to simulate the natural conditions found in the earth's crust to artificially synthesize a variety of materials and morphology, such as iron oxides (the focus of our review), in the laboratory.[90–92]

It is well known that iron salts can generate iron oxides in appropriate conditions, producing hematite and goethite from amorphous iron(III) hydroxide at an elevated temperature at a different pH.[93] To produce iron oxides under hydrothermal conditions, the pH of the aqueous solutions and the temperature seem to play an important role and must be carefully controlled. As an example, the most common material phases obtained from hydrolysis of aqueous iron chloride ($FeCl_3$) solution, oxyhydroxides such as goethite (α-FeOOH), akaganeite (β-FeOOH), and

https://doi.org/10.1557/jmr.2013.302 Published online by Cambridge University Press

eventually direct pure hematite (α-Fe_2O_3), can be reached at specific conditions.[94] For instance, the formation of goethite preferentially occurs at an alkaline pH (8–11), and from a 100 to 200 °C temperature range, hematite also can eventually be formed. The equation of the stable solid phase's formation is shown as below, which reflects the relatively simple nucleation of each phase and the transformation of goethite in hematite[94]:

$$\mathrm{Fe(III)(aq)} \rightarrow \mathrm{Fe_2O_3 \cdot xH_2O} \rightarrow \alpha - \mathrm{FeOOH} \rightarrow \alpha - \mathrm{Fe_2O_3} \quad . \qquad (3)$$

Particularly, the aqueous solution at a pH range of 0.8–2.6, kept around 100 °C, forms akaganeite, whereas at a higher temperature, only hematite is expected as the reaction product.

In the next topic, iron oxide films produced in hydrothermal conditions on the transparent conductor glass substrate (FTO) with controllable morphology composed by vertically aligned nanorods, first reported by Vayssieres et al.[85,95,96] and named as PBM will be addressed. This iron oxide nanorod arrays supported on the FTO conductor glass substrate has attracted the academic and industrial community because of its potential application as a photoanode in PEC cells to generate alternative, clean, and sustainable fuels.

B. Undoped vertical hematite nanorod electrodes

Early works related to the preparation of material in hydrothermal conditions were done using appropriate equipment (such as autoclaves) at high temperature and pressure. However, in search of methods to achieve more practical and capable approach for producing nanostructures with controlled morphology, Vayssieres et al.[85,95,96] developed a method called PBM. Along these two decades, innumerous variations of the PBM process were proposed to improve the quality, reproducibility, and properties of the synthesized materials. As aforementioned, here we will focus only the improvements reached on photocatalytic performance of the iron oxide nanostructure (hematite) grown on the conductor glass substrate (FTO) by the PBM method, simulating a photoanode in the PEC cell.[96–98] Generally, synthesis of iron oxide performed under hydrothermal conditions at low temperatures results in FeOOH, the hydrated phase of iron oxide (akaganeite and/or goethite), being necessarily an additional treatment at elevated temperature to obtain pure and active hematite electrodes. The original PBM process can be easily described by the preparation of an aqueous solution containing ferric chloride ($FeCl_3 \cdot 6H_2O$) and sodium nitrate ($NaNO_3$) set at pH 1.5 (using HCl) in an autoclavable screw cap. An interesting insight given by the authors was the immersion of the transparent conductor glass substrate (FTO) for directly producing nanostructured films. To obtain substrates with iron oxide layers composed of vertically aligned rods (in nanoscale), the precursor solution was kept during 24 h at 100 °C in a regular oven. The final product of the synthesis is a film with a large covered area by vertically aligned nanorod arrays on the FTO conductor glass substrate in the hydrated phase of iron as depicted in Fig. 2.

Hagfeldt et al.[60,99] used this novel concept of vertical nanorod array films showing significant improvements in photoelectrohemical performance compared with other hematite film morphologies.[25,51] It is worth mentioning that to obtain films in the hematite phase from the PBM method, an additional thermal treatment at 550 °C for 1 h was conducted; however, no drastic changes were observed on that morphology, as illustrated in Fig. 2. The enhancement of photocurrent response was related to the morphology constituted by vertically aligned hematite nanorods with a sufficiently small diameter (4–5 nm)[100] close to the diffusion length of a photogenerated hole (2–4 nm).[28,30] This means that the poor hematite hole transport can be overcome using a morphology composed of sufficiently narrow wires or rods, ensuring the proximity of the diffusion length to reach the hematite surface and oxidize water before the recombination.[17] Moreover, they showed that the wires and rods with very narrow radii can present one-dimensional quantum confinement, manifesting a significant blue-shift and making feasible the direct reduction of water without additional external bias. This is possible due the upward shift of the conduction band; however, using hematite as a photoanode to split water without the assistance of an external bias was not yet reported.[17,100] It is interesting to note that since the first studies done by Vayssieres et al., significant improvement for pure hematite was only reported almost 10 years later.

In 2011, a significant improvement in photocatalytic performance due to the activation of hematite surfaces interpreted by the use of appropriated annealing conditions

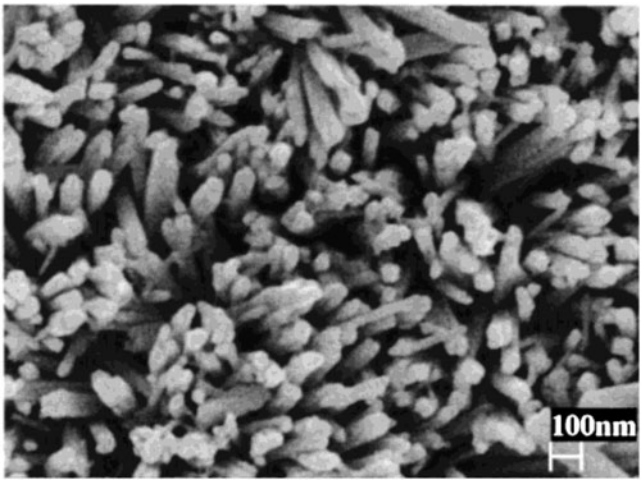


FIG. 2. SEM micrographs of oriented self-assembled bundles of β-FeOOH/hematite nanorods onto FTO substrates synthesized by the PBM process. Reprinted with permission from Ref. 96. Copyright 2001, American Chemical Society.

https://doi.org/10.1557/jmr.2013.302 Published online by Cambridge University Press

was reported in revisiting the PBM method.[101] For photoeletrochemical characterization, an aqueous electrolyte solution of 1 M NaOH and 450 W xenon lamp sunlight simulator coupled with AM 1.5G filter were used. The light intensity was set to 87 mW/cm^2, and the illuminated electrode area was 0.95 cm^2. The hematite electrodes annealed at 700 °C, and further at 750 °C for 5 min showed a photocurrent around 0.52 mA/cm^2 at 1.23 V_{RHE} under standard illumination. Alternatively, the hematite treated at a lower temperature (600 °C) for an extended time exhibited photocatalytic improvements at levels intermediate to the 5-min treatments at 700 and 750 °C.[101] In addition, the pure hematite electrodes displayed the lowest onset potentials around +0.75 V_{RHE} compared to many reports.[39,82,102–104] The reduction of onset potentials may indicate that the annealed hematite electrode contained very few surface-trapping states and consequently increase the electron collection or reduce the recombination rate (pair electron–hole).[28,42] The hematite electrode achievements were attributed to the morphology changes, where the grains apparently coalesced, presenting a very smooth surface. Based on a recent discussion, the surface morphology caused by high temperature thermal treatment could act favoring the (photo) electron transfer along nanostructures to back contact, and aid the (photo) hole to reach the surface.[105] Hematite electrodes produced by other strategies with a variety of morphologies exposed at a higher temperature also show photocatalytic enhancement.[34,64]

One year later, another interesting improvement in the hematite PEC performance produced by the PBM method was reached by activating the hematite surface during thermal treatment in the presence of controlled oxygen content.[106] In this study, the samples were thermally treated at 550 °C for 2 h in an oxygen-deficient atmosphere (N_2 + air) to promote oxygen vacancies in air with certain oxygen content. As previously discussed, for many authors, the thermal activation treatment did not change the nanorod or wire morphology. The hematite sample treated in oxygen-deficient atmosphere displayed enhanced photocurrent density compared with hematite prepared in air. The PEC performance was conducted illuminating in front side 0.15 cm^2 of working area using a solar simulator (Newport 69920, 1000 W xenon lamp, Oriel Instruments, Stratford, CT) coupled with an infrared water filter (Oriel 6127, Oriel Instruments, Stratford, CT) and an AM 1.5 global filter (Newport 81094, Oriel Instruments, Stratford, CT). The light intensity was set to 100 mW/cm^2 using a power meter (Molectron, PM5100, Molectron Detector, Inc., Portland, OR). The improved hematite photocurrent response of 1.82 mA/cm^2 at 1.23 V_{RHE} with a maximum value of around 3.37 mA/cm^2 at 1.50 V_{RHE} was attributed to the increased donor density resulting from the formation of VO (Fe^{2+}).[106] In fact, the photocurrent was increased by thermal treatment in the presence of oxygen atmosphere; however, the water photooxidation is observed at high overpotential around 1.0 V_{RHE}.

In the same year, it was showed that even with the time of synthesis reduced from 24 (originally proposed) to 6 h, a homogenous iron oxide nanorod distribution can be observed [Fig. 3(a)] covering a large area of the substrate.[82] After treatment at 390 °C for 1 h, the films presented a photocurrent response of around 0.9 mA/cm^2 at 1.4 $V_{RHE,}$ with a maximum value of 3.0 mA/cm^2 at 1.6 $V_{RHE.}$ The onset potential at 1.37 V_{RHE} was found for this material [Fig. 3(b)]. As previously discussed, the high value of onset potential has been attributed to the presence of defects on the hematite surface reducing the rate of charge transfer along of the nanostructure, consequently increaseing the recombination rate. The promising photoeletrochemical performance must have an efficient solid–solid interface (hematite layer and conductor substrate) for avoiding a fast recombination between the photogenerated electron–hole pair.

Moreover, the authors studied the water oxidation reaction, considered as a major challenge to be overcome

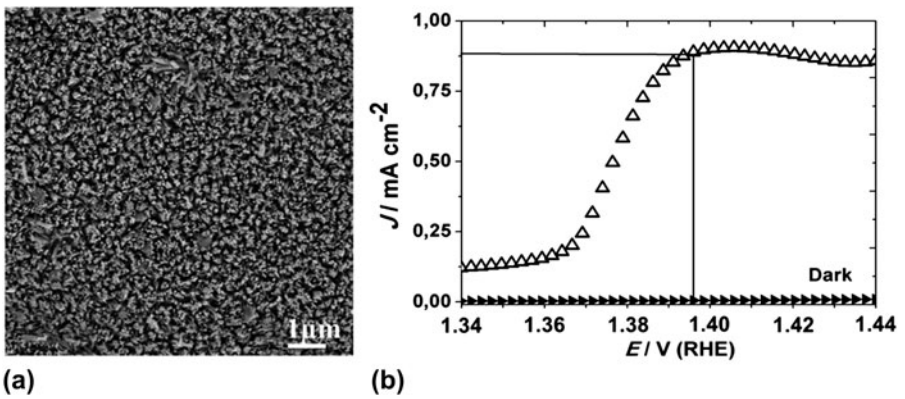


FIG. 3. (a) Top-view of SEM images of vertical hematite nanorods; (b) current density versus voltage (RHE) curves under dark and illuminated conditions for vertical hematite nanorods thermally treated at 390 °C for 1 h. Ozone-free xenon lamp coupled to AM 1.5 global filters. Electrolyte 1 M NaOH (set at pH 13.6).

https://doi.org/10.1557/jmr.2013.302 Published online by Cambridge University Press

and understanding in the area. From the cyclic voltammetry results, an important step in explaining the mechanism of evolution of molecular oxygen onto vertically oriented nanorod hematite surfaces was presented. The researchers assumed that the molecular oxygen evolution was preceded by the formation of an oxyhydroxide group on the electrode/electrolyte interface, seen as a slow and possibly limiting step. The Eqs. (4) and (5) below summarize the proposed steps on the oxygen evolution reaction (OER) mechanism on the hematite surface:

Step1: OH^- adsorption (slow)

$$4\alpha - Fe_2O_3 + 4OH^- \rightarrow 4\alpha - Fe_2O_3(OH)^-_{ads} \quad . \quad (4)$$

Step2: molecular oxygen evolution ($E = 0.38$ V)

$$4\alpha - Fe_2O_3(OH)^-_{ads} + 4h\nu \rightarrow 4\alpha - Fe_2O_3 + \uparrow O_2 + 2H^+ + 2H_2O + 2e^- \quad . \quad (5)$$

Usually, the OH^- adsorption process on the metal oxide surface is governed by a Nernstian equilibrium (already observed for TiO_2).[107–111]

Later, this OER mechanism was confirmed to be strictly dependent on the OH^- group concentration and playing an important role in shifting the water oxidation to a lower positive potential.[83] In addition, the impact of different temperatures of thermal treatment on the electrochemical and photoeletrochemical properties of vertical hematite nanorod arrays was discussed. For hematite films thermally treated at temperatures higher than 400 °C, the photocurrent response displayed a negligible response, indistinguishable from the dark current on the range measured. The unexpected PEC response of films treated at a high temperature compared with the literature can be related to morphology and crystallographic orientation.[83] The high temperature of thermal treatment could not be enough to eliminate the major content of defects on the morphology, meaning that the presence of defects increases the electron–hole recombination rate, reducing the hematite performance. An example of this morphology is illustrated in Fig. 4(a), electronic transmission microscopy images showing a view of nanorods thermally treated at 800 °C, at which it is possible to observe a polycrystalline rod. In the case of crystallographic orientation, the high temperature of thermal treatment could alter the preferential orientation of the crystal, compromising the efficiency of electron transport, as represented in Fig. 4(b).

Another alternative proposed in 2012 was the introduction of lattice defects into pure hematite composed of vertical nanorods by adding inorganic salts to enhance the PEC performance. Lattice defects are expected to act in hematite to decrease the flat band potential from 0.63 to 0.58 V_{RHE} and increase the carrier density from 1.83×10^{20} to 5.44×10^{20} cm^{-3}, consequently reducing the oxygen evolution potential and enhancing the PEC

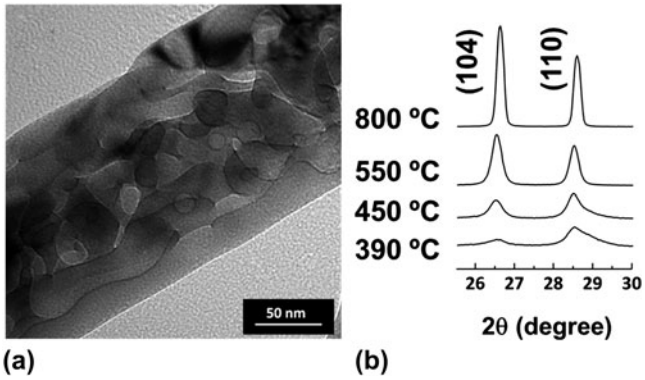


FIG. 4. (a) Electronic transmission microcopy image of a vertical hematite nanorod sintered at 800 °C for 15 min; (b) zoom of x-ray diffraction curve exhibiting the evolution of preferential crystallographic orientation with different temperatures of sintering for vertical hematite nanorods.[112]

performance. Actually, a significant photocurrent density (1.2 mA/cm^2) was only achieved at the higher onset potential 1.6 V_{RHE}. Nevertheless, the introduction of lattice defects on the hematite surface can be an alternative way to improve the photocatalytic performance than inclusion of dopant.[97]

In fact, a consensus is seen in the literature that hematite electrodes sintered at a high temperature is an efficient way to obtain materials for PEC cells, independent of the method used to produce them.[65] Moreover, concomitant of the advances presented above for pure hematite electrodes, significant studies demonstrate that the coupling of the vertical hematite nanorod electrode with oxygen catalysts can play a distinct role in enhancing PEC activity. For instance, oxygen catalysts as a dopant can reduce the overpotential required to oxidize water.[107,113]

C. Doped vertical hematite nanorod electrodes

The insertion of a variety of elements such as Si, Sn, Pt, Ti, etc. as dopants is known to lead to enhanced photocatalytic activity of the hematite photoanode produced for any method.[39,48,62,114–118] As mentioned above, hematite films prepared under hydrothermal conditions enable efficient coverage of a large area of different kinds of substrates, allowing modifications during materials processing. Among these modifications, doping metal oxide films with any elements via the hydrothermal process is also considered a simple alternative to improve the performance of PEC.

For instance, the intentional insertion or diffusion from the FTO conductor glass substrate of Sn during the synthetic process of vertically aligned hematite nanorods or the use of high-temperature sintering can give an effective gain in electronic properties.

Vertical hematite nanorod thermally treated at 550 °C for 2 h and additionally treated at a higher temperature (e.g., 800 °C) for 20 min was investigated. From x-ray

https://doi.org/10.1557/jmr.2013.302 Published online by Cambridge University Press

diffraction (XRD) and scanning electron microscopy (SEM) results, no changes in the morphology in either the structural or crystal phase can be observed after high-temperature sintering (800 °C), as previously discussed here. However, by x-ray photoelectron spectroscopy analysis, the presence of Sn from the FTO conductor glass substrate by a diffusion process during the hematite nanorod film sintering was found. The photoeletrochemical response was recorded using a solar simulator (Newport, model 69907) coupled to a filter (AM 1.5G) using a 150-W xenon lamp as the white light source. The illuminated area was 0.12 cm^2 with a light power density of 100 mW/cm^2. A better photocurrent response was found for films treated at a higher temperature (800 °C), approximately 1.24 mA/cm^2 at 1.23 V_{RHE} with a maximum around 1.95 mA/cm^2 at 1.6 V_{RHE} exhibiting a very low onset potential between 0.6 and 0.7 V_{RHE}.[36] Hematite synthesized using the same procedure with the intentional addition of tin (IV) chloride as a source of Sn, and sintered at a different temperature, also changed the electronic properties. At 800 °C, both situations described displayed approximately the same Sn percentage and high photocurrent response starting at low onset potential. Sn doping in the initial stage of hematite preparation showed a higher PEC performance and drastic change in morphology, attributed to the smaller feature size of nanocoral obtained in the second case, consequently exhibiting a high active surface area.[36] A flat band potential around 0.49 V_{RHE} and donor density between 1.89×10^{19} and 5.38×10^{19} cm^{-3} were extracted from Mott–Schottky plots (samples treated from 650 to 800 °C). Usually, one strategy used to identify the insertion of dopants on the semiconductor is examining changes in the concentration of charge carrier density. As aforementioned, these results confirmed the presence of Sn on the hematite photoanode prepared by different strategies allied with high-temperature sintering and can be used to enhance the hematite performance on PEC cells.[36,37,65]

Another promising set of dopants based on Ni and Co oxygen evolution catalysts (OEC) on hematite nanorods has been used as a simple strategy to improve the photoresponse and shift the onset potential required to oxidize water in a PEC cell close to the flat band potential of hematite.[16,18,107,114,118,119] Following this strategy, Co–Pi and Ni–Bi thin catalyst layers were inserted in vertically aligned hematite nanorod films. As expected, the Co–Pi OEC exhibited an overall improvement on the PEC performance, showing a prominent onset potential reduction, whereas the Ni–Bi OEC displayed a significant photoresponse close to the flat band potential of hematite, with gradual reduction of performance at higher overpotential for reasons not yet elucidated.[120]

An element commonly used as a catalyst is platinum. The inclusion of Pt on hematite improves the photoinduced conductivity and enhances charge transfer by suppressing a carrier recombination due to the substitution of Pt^{4+} for Fe^{3+} as electron donor. Pt-doped hematite has enhanced photocurrent density from 1.2 to 1.38 mA/cm^2 at 1.23 V_{RHE} under 1 sun illumination. The flat band potential was around −0.78 $V_{Ag/AgCl}$ and the charge carrier density was found to be 1.1×10^{21} cm^{-3} at 3 kHz for samples.[121] It is worth mentioning that the temperature used for sintering the Pt-doped hematite was 170 °C, relatively low compared with what is usually reported.

Recently, a novel design of heterojunction arrays of hematite nanorod being cores (produced by the hydrothermal process onto the Ti substrate), with graphene acting as an interlayer, and $BiV_{1-x}Mo_xO_4$ as shells both deposited by a spin-coating technique was investigated.[122] The heterojunction arrays exhibit a pronounced photocurrent density of 1.97 mA/cm^2 at 1.0 $V_{Ag/AgCl}$, and photoconversion efficiency around 0.53% at −0.04 $V_{Ag/AgCl}$. The PEC enhancement was achieved due to high light absorption between hematite cores—$BiV_{1-x}Mo_xO_4$ shell interaction, and also due to more efficient photogenerated electron–hole pair separation on the heterojunction array interfaces mediated by graphene (Fig. 5).

More recently, a new direction was pointed out for producing highly efficient vertical hematite nanorod electrodes. The proposed strategy is based on hematite nanorod changes in synthesis and surface treatment.[123]

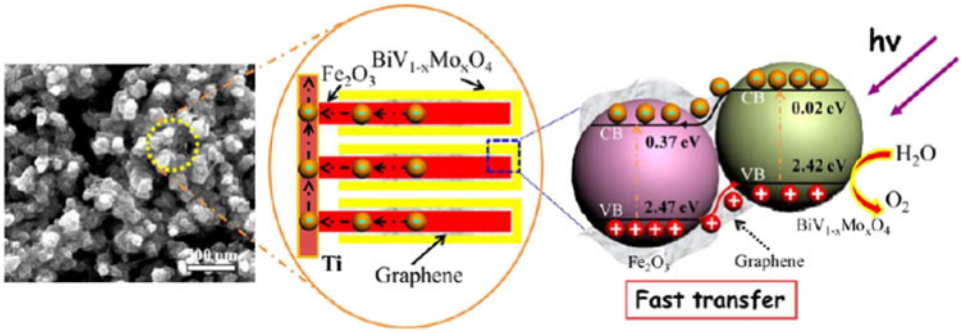


FIG. 5. Heterojunction of hematite nanorod arrays (cores) prepared under hydrothermal conditions modified by graphene (interlayer) and $BiV_{1-x}Mo_xO_4$ actuated as shells deposited by a spin-coating technique. Reprinted with permission from Ref. 122. Copyright 2012, American Chemical Society.

https://doi.org/10.1557/jmr.2013.302 Published online by Cambridge University Press

First, hematite is synthesized, modifying the concentration of chloride in the precursor solution to change the $NaNO_3$ and HCl from the original PBM method to urea and, after few hours under hydrothermal conditions, the iron oxyhydroxide phase composed of nanorod arrays was obtained. Second, before the sintering process, at 750 °C for 30 min in air, 5 to 20 mmol/L of Sn(IV) in an aqueous solution was uniformly dropped on the film surface to penetrate all covered areas. During the sintering process, a solid-state diffusion reaction Sn(IV) was gradually incorporated, forming a thin layer of SnO_2 coating the hematite rods.[124] In a previous study, the possible excess of SnO_2 on the surface was removed by NaOH treatment, and as a consequence, a very thin layer of $Fe_xSn_{1-x}O_4$ could be formed on the surface and remains unaffected by repeating this treatment.[125]

For the PEC experiment, a light source was simulated sunlight from a 150-W xenon solar simulator (67005, Newport corporation) through a solar filter with a measured intensity equivalent to standard AM 1.5 sunlight (100 mW/cm^2) at the sample face. The highest photocurrent value of 2.25 mA/cm^2 at 1.23 V_{RHE} was found for hematite nanorod films modified with 20 mmol/L of Sn(IV) and treated at 750 °C for 30 min. Additionally, a shift in the low onset potential at 100 mV, improvements in IPCE, and an increase in the efficiency of oxygen evolution were observed. Xi et al.[73] attributed their improvements to the very thin layer of tin oxide coating the hematite rods, reducing surface defects, increasing the charge injection efficiency and avoiding a fast electron–hole recombination at hematite nanorod–electrolyte interface.

These changes to the original PBM synthetic process opened new perspectives and opportunities for understanding the real role of urea, as well as the effect of a thin layer of tin oxide and eventually enabling the process for commercial applications. Revisiting the strategy adopted by Wong changing from 10 to 2 h the period of synthesis, a pure and modified hematite (tin oxide layer) photoanodes showed a significant enhancement (Fig. 6).

The photocurrent density of undoped hematite photoanode performed in the dark (solid line curve) and under stander illuminated conditions (dash dot and dash line curve) using aqueous electrolyte with 1 M NaOH (set at pH 13.6) exhibited a value of 1.40 mA/cm^2 at 1.23 V_{RHE} with the overpotential at around 0.95 V_{RHE}. Although the photocurrent response is slightly higher than the value reported for undoped hematite photoanode (PBM), the overpotential around 0.95 V_{RHE} is far from an ideal for favoring electrochemical reaction. To understand the impact of the overpotential on photocurrent response on the n-type semiconductor, the PEC experiment was conducted in the presence of a "hole scavenger" like H_2O_2. This strategy has been pointed as a useful tool for diagnosing the limitations of high performance.[105] The current density response of vertically aligned nanorod hematite photoanode in the presence of hole scavenger (in dark and under illuminated standard conditions, dotted and solid green curves, Fig. 6) exhibited a high photocurrent value of 1.8 mA/cm^2 at 1.23 V_{RHE} with lower overpotential value of 0.75 V_{RHE}. This experiment illustrated in Fig. 6 is in agreement with many investigations reported in the literature examining different hematite nanostructures produced by several strategies. The plausible explanation for a superior photocurrent response observed in this condition must be related to the shift in the overpotential. This means that since the photogenerated hole is available for oxidation, the rate of water oxidation can be very low limiting hematite photocurrent response.[105,126,127] From these results using H_2O_2, a real perspective is open to find a way to improve the hematite photocurrent response produced by several methods including the PBM process.

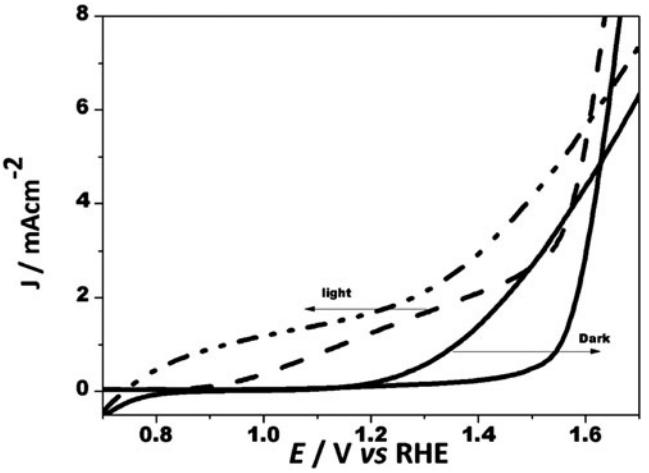


FIG. 6. Photocurrent density versus voltage (Ag/AgCl$_{sat}$) curves under dark (solid line curves) and illuminated (dash dot and dash lines) conditions for undoped vertical hematite nanorods photoanode synthesized by the PBM process during 2 h and thermally treated at 750 °C for 30 min. Ozone-free xenon lamp coupled to AM 1.5 global filters. Electrolyte 1 M NaOH (set at pH 13.6) and 1 M NaOH + 0.5 M H_2O_2.

For instance, incorporating a thin layer of tin oxide on the hematite films produced at 2 h and heat treated at 750 °C for 30 min, a superior photocurrent was observed. The photocurrent density was found at around 2.61 mA/cm^2 at 1.23 V_{RHE}, as illustrated in Fig. 7 (left). As aforementioned, concomitant with a high photocurrent value, the onset potential (~0.8 V_{RHE}) was shifted to lower values, making the modified vertical hematite nanorod a more efficient material for oxidizing water.[123] Generally, the Mott–Schottky plots are used to elucidate the role of the insertion of a dopant on a semiconductor material, which changes the concentration of the charge carrier (ex. N_d). Particular attention should be given for estimating the N_d from Mott–Schottky plots for electrodes with a morphology composed by nanorods because the space charge regions is not similar to planar electrodes.[28,123,128] The addition of Sn(IV) to vertical hematite nanorod electrodes was found to increase the donor density (N_d) from 10^{18} for pure hematite to 10^{20} cm^{-3} (modified with Sn) both at

https://doi.org/10.1557/jmr.2013.302 Published online by Cambridge University Press

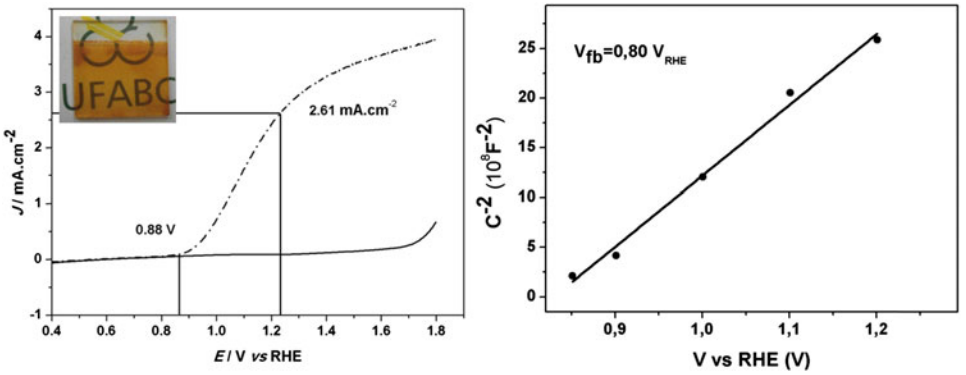


FIG. 7. Left: current density versus voltage (RHE) curves under dark (solid line) and illuminated (dash line) conditions for vertical hematite nanorod photoanode doped with 20-mM Sn(IV) thermally treated at 750 °C for 30 min. Ozone-free xenon lamp coupled to AM 1.5 global filters. Electrolyte 1 M NaOH (set at pH 13.6).

a frequency of 1 KHz. Contrary to this value found by Wong et al., for a higher photocurrent value presented in Fig. 7 (left), the donor density (N_d) was 9.05×10^{17} cm^{-3} estimated at a frequency of 1 KHz [see Fig. 7 (right)].

However, the flat band potential (V_{fb}) was estimated to be around 0.8 V_{RHE} [Fig. 7 (right)]. Both results combined (N_d and V_{fb}), meaning that the space charge region width (W) could be slightly higher, favoring the charge separation at the space charge region. In addition, allied to the description above, the formation of a thin layer of Sn coating the hematite nanorod can increase the efficiency of the electron injection, which could be a reasonable explanation for the photocatalytic enhancement observed in Fig. 7 (Left). In addition, for undoped investigation in the presence of a hole scavenger, the close values of the overpotential and flat band potential suggest that the available photogenerated holes present at the solid–liquid surface junction are being efficiently used for water photooxidation. Finally, the high temperature of sintering is an important requirement for hematite films produced by any synthetic route, and a dopant working in harmony with the morphology can be very useful for obtaining efficient materials for PEC cells. In addition, Xi et al.[123] strategy gives new opportunities to improve the vertical hematite nanorod as photoanode.

III. SUMMARY

After 10 years, since was first used, the vertical hematite nanorod produced by the PBM process seems to have achieved important advances. To find ways for improving the photoacatalytic performance of "PBM hematite," innumerous works were investigated focusing on the electronic properties, doping effect, prelayer, and hematite surfaces activation using temperature. However, the real perspective for the use of the PBM process was only recently presented by Wong et al., where they proposed efficient changes to the original method. The strategy consisted in the use of urea during the initial stage of the synthesis, and the tin oxide layer deposited before thermic treatment seems to play in great harmony increasing the photocurrent and concomitant reducing the overpotential. This means that both alteration done in the original PBM process was attributed to reduce the recombination rate at the solid–liquid junction allied with a more efficient electron injection at back contact (substrate) favoring the electrochemical reaction in both electrodes. In the present manuscript, this novel strategy was revisited and the results clearly confirm the real perspectives for improving the PEC performance of hematite electrodes. In fact, the investigation carried out in undoped hematite in the presence of hole scavenger (H_2O_2) and in its absence clearly showed the possibility for enhancing its photocatalytic performance. For instance, with addition of the tin oxide layer on the hematite nanorod before the thermal treatment, following the Wong strategy, a superior photocurrent response with low overpontential compared with undoped material was obtained. It is worthmentioning that the undoped and modified hematite electrodes presented in this work show a superior performance inclusive comparing with results shown by Wong. Additionally, a complementary discussion about the use of a novel PBM strategy and the effect of the tin oxide layer on the hematite electrode was pointed out. Then, since there are many possibilities to overcome hematite limitations, new advances in the use of vertical hematite nanorods have gained a significant foothold allying favorable morphology and active surface with a simple and inexpensive way to produce a large-area electrode. Further, investigation on identifying and understanding a remarkable strategy to activate the hematite nanorod surface and making possible the use of the PBM process interesting for commercial applications will be addressed in the future.

ACKNOWLEDGMENTS

We gratefully acknowledge financial support from the Brazilian agencies of FAPESP (Grant Nos. 2011/19924-2,

https://doi.org/10.1557/jmr.2013.302 Published online by Cambridge University Press

2012/19926-8, and 2013/07296-2), CAPES, CNPq (Grant No. 555855/2010-4), InstitutoNacionalemEletrônicaOrgânica (INEO), NanoBioMed Brazil Network (CAPES), and INCTMN.

REFERENCES

1. A. Fujishima and K. Honda: Electrochemical photolysis of water at a semiconductor electrode. *Nature* **238**(5358), 37 (1972).
2. A.J. Bard, G.M. Whitesides, R.N. Zare, and F.W. McLafferty: Holy grails of chemistry. *Acc. Chem. Res.* **28**(3), 91 (1995).
3. S.S. Mao, S. Shen, and L. Guo: Nanomaterials for renewable hydrogen production, storage and utilization. *Prog. Nat. Sci.* **22**(6), 522 (2012).
4. K. Sivula, F. Le Formal, and M. Grätzel: Solar water splitting: Progress using hematite (α-Fe_2O_3) photoelectrodes. *ChemSusChem* **4**(4), 432 (2011).
5. Y. Tachibana, L. Vayssieres, and J.R. Durrant: Artificial photosynthesis for solar water-splitting. *Nat. Photon.* **6**(8), 511 (2012).
6. X. Liu, F. Wang, and Q. Wang: Nanostructure-based WO_3 photoanodes for photoelectrochemical water splitting. *Phys. Chem. Chem. Phys.* **14**(22), 7894 (2012).
7. S.H. Baeck, K.S. Choi, T.F. Jaramillo, G.D. Stucky, and E.W. McFarland: Enhancement of photocatalytic and electrochromic properties of electrochemically fabricated mesoporous WO_3 thin films. *Adv. Mater.* **15**(15), 1269 (2003).
8. R.H. Gonçalves, L.D.T. Leite, and E.R. Leite: Colloidal WO_3 nanowires as a versatile route to prepare a photoanode for solar water splitting. *ChemSusChem* **5**(12), 2341 (2012).
9. X. Zhang, X. Lu, Y. Shen, J. Han, L. Yuan, L. Gong, Z. Xu, X. Bai, M. Wei, Y. Tong, Y. Gao, J. Chen, J. Zhou, and Z.L. Wang: Three-dimensional WO_3 nanostructures on carbon paper: Photoelectrochemical property and visible light driven photocatalysis. *Chem. Commun.* **47**(20), 5804 (2011).
10. H. Wang, T. Deutsch, and J.A. Turner: Direct water splitting under visible light with nanostructured hematite and WO_3 photoanodes and a $GaInP_2$ photocathode. *J. Electrochem. Soc.* **155**(5), F91 (2008).
11. A.J. Cowan, J. Tang, W. Leng, J.R. Durrant, and D.R. Klug: Water splitting by nanocrystalline TiO_2 in a complete photoelectrochemical cell exhibits efficiencies limited by charge recombination. *J. Phys. Chem. C* **114**(9), 4208 (2010).
12. M. Ni, M.K.H. Leung, D.Y.C. Leung, and K. Sumathy: A review and recent developments in photocatalytic water-splitting using TiO_2 for hydrogen production. *J. Renewable Sustainable Energy* **11**(3), 401 (2007).
13. B. Klahr, S. Gimenez, F. Fabregat-Santiago, T. Hamann, and J. Bisquert: Water oxidation at hematite photoelectrodes: The role of surface states. *J. Am. Chem. Soc.* **134**(9), 4294 (2012).
14. T.W. Hamann: Splitting water with rust: Hematite photoelectrochemistry. *Dalton Trans.* **41**(26), 7830 (2012).
15. A. Hagfeldt and M. Grätzel: Light-induced redox reactions in nanocrystalline systems. *Chem. Rev.* **95**(1), 49 (1995).
16. J. Sun, D.K. Zhong, and D.R. Gamelin: Composite photoanodes for photoelectrochemical solar water splitting. *Energy Environ. Sci.* **3**(9), 1252 (2010).
17. R. van de Krol, Y. Liang, and J. Schoonman: Solar hydrogen production with nanostructured metal oxides. *J. Mater. Chem.* **18**(20), 2311 (2008).
18. M. Dinca, Y. Surendranath, and D.G. Nocera: Nickel-borate oxygen-evolving catalyst that functions under benign conditions. *Proc. Natl. Acad. Sci. U.S.A.* **107**(23), 10337 (2010).
19. L. Andrade, T. Lopes, H.A. Ribeiro, and A. Mendes: Transient phenomenological modeling of photoelectrochemical cells for water splitting – application to undoped hematite electrodes. *Int. J. Hydrogen Energy* **36**(1), 175 (2011).
20. K. Maeda: Photocatalytic water splitting using semiconductor particles: History, and recent developments. *J. Photochem. Photobiol., C* **12**(4), 237 (2011).
21. Y. Li and J.Z. Zhang: Hydrogen generation from photoelectrochemical water splitting based on nanomaterials. *Laser Photon. Rev.* **4**(4), 517 (2009).
22. B.D. Alexander, P.J. Kulesza, I. Rutkowska, R. Solarska, and J. Augustynski: Metal oxide photoanodes for solar hydrogen production. *J. Mater. Chem.* **18**(20), 2298 (2008).
23. A.B. Murphy, P.R.F. Barnes, L.K. Randeniya, I.C. Plumb, I.E. Grey, M.D. Horne, and J.A. Glasscock: Efficiency of solar water splitting using semiconductor electrodes. *Int. J. Hydrogen Energy* **31**(14), 1999 (2006).
24. K.L. Hardee: Semiconductor electrodes: V. The application of chemically vapor deposited iron oxide films to photosensitized electrolysis. *J. Electrochem. Soc.* **123**(7), 1024 (1976).
25. J.H. Kennedy: Photooxidation of water at α-Fe_2O_3 electrodes. *J. Electrochem. Soc.* **125**(5), 709 (1978).
26. M.P. Dare-Edwards, J.B. Goodenough, A. Hamnett, and P.R. Trevellick: Electrochemistry and photoelectrochemistry of iron(III) oxide. *J. Chem. Soc. Faraday Trans.* **79**(9), 2027 (1983).
27. C.M. Eggleston: Geochemistry. Toward new uses for hematite. *Science* **320**(5873), 184 (2008).
28. M.G. Walter, E.L. Warren, J.R. McKone, S.W. Boettcher, Q. Mi, E.A. Santori, and N.S. Lewis: Solar water splitting cells. *Chem. Rev.* **110**(11), 6446 (2010).
29. B.M. Klahr and T.W. Hamann: Voltage dependent photocurrent of thin film hematite electrodes. *Appl. Phys. Lett.* **99**(6), 063508 (2011).
30. M.J. Katz, S.C. Riha, N.C. Jeong, A.B.F. Martinson, O.K. Farha, and J.T. Hupp: Toward solar fuels: Water splitting with sunlight and "rust"? *Coord. Chem. Rev.* **256**(21–22), 2521 (2012).
31. N. Iordanova, M. Dupuis, and K.M. Rosso: Charge transport in metal oxides: A theoretical study of hematite alpha-Fe_2O_3. *J. Chem. Phys.* **122**(14), 144305 (2005).
32. K. Shimizu, A. Lasia, and J-F. Boily: Electrochemical impedance study of the hematite/water interface. *Langmuir* **28**(20), 7914 (2012).
33. J. Liu, M. Shahid, Y.S. Ko, E. Kim, T.K. Ahn, J.H. Park, and Y.U. Kwon: Investigation of porosity and heterojunction effects of a mesoporous hematite electrode on photoelectrochemical water splitting. *Phys. Chem. Chem. Phys.* **15**(24), 9775 (2013).
34. J. Brillet, M. Grätzel, and K. Sivula: Decoupling feature size and functionality in solution-processed, porous hematite electrodes for solar water splitting. *Nano Lett.* **10**(10), 4155 (2010).
35. R.H. Gonçalves, B.H.R. Lima, and E.R. Leite: Magnetite colloidal nanocrystals: A facile pathway to prepare mesoporous hematite thin films for photoelectrochemical water splitting. *J. Am. Chem. Soc.* **133**(15), 6012 (2011).
36. Y. Ling, G. Wang, D.A. Wheeler, J.Z. Zhang, and Y. Li: Sn-doped hematite nanostructures for photoelectrochemical water splitting. *Nano Lett.* **11**(5), 2119 (2011).
37. C.X. Kronawitter, I. Zegkinoglou, C. Rogero, J.H. Guo, S.S. Mao, F.J. Himpsel, and L. Vayssieres: On the interfacial electronic structure origin of efficiency enhancement in hematite photoanodes. *J. Phys. Chem. C* **116**(43), 22780 (2012).
38. F.L. Souza, K.P. Lopes, P.A.P. Nascente, and E.R. Leite: Nanostructured hematite thin films produced by spin-coating deposition solution: Application in water splitting. *Sol. Energy Mater. Sol. Cells* **93**, 362 (2009).
39. I. Cesar, A. Kay, J.A. Gonzalez Martinez, and M. Grätzel: Translucent thin film Fe_2O_3 photoanodes for efficient water

https://doi.org/10.1557/jmr.2013.302 Published online by Cambridge University Press

splitting by sunlight: Nanostructure-directing effect of Si-doping. *J. Am. Chem. Soc.* **128**(14), 4582 (2006).
40. A. Kay, I. Cesar, and M. Grätzel: New benchmark for water photooxidation by nanostructured alpha-Fe_2O_3 films. *J. Am. Chem. Soc.* **128**(49), 15714 (2006).
41. S.D. Tilley, M. Cornuz, K. Sivula, and M. Grätzel: Light-induced water splitting with hematite: Improved nanostructure and iridium oxide catalysis. *Angew. Chem. Int. Ed.* **122**(36), 6549 (2010).
42. N.T. Hahn and C.B. Mullins: Photoelectrochemical performance of nanostructured Ti-and Sn-doped α-Fe_2O_3 photoanodes. *Chem. Mater.* **22**, 6474 (2010).
43. J. Frydrych, L. Machala, J. Tucek, K. Siskova, J. Filip, J. Pechousek, K. Safarova, M. Vondracek, J.H. Seo, O. Schneeweiss, M. Grätzel, K. Sivula, and R. Zboril: Facile fabrication of tin-doped hematite photoelectrodes: Effect of doping on magnetic properties and performance for light-induced water splitting. *J. Mater. Chem.* **22**(43), 23232 (2012).
44. J.A. Glasscock, P.R.F. Barnes, I.C. Plumb, and N. Savvides: Enhancement of photoelectrochemical hydrogen production from hematite thin films by the introduction of Ti and Si. *J. Phys. Chem. C* **111**(44), 16477 (2007).
45. C. Sanchez, K.D. Sieber, and G.A. Somorjai: The photoelectrochemistry of niobium doped α-Fe_2O_3. *J. Electroanal. Chem.* **252**(2), 269 (1988).
46. T. Hisatomi, H. Dotan, M. Stefik, K. Sivula, A. Rothschild, M. Grätzel, and N. Mathews: Enhancement in the performance of ultrathin hematite photoanode for water splitting by an oxide underlayer. *Adv. Mater.* **24**(20), 2699 (2012).
47. T. Hisatomi, J. Brillet, M. Cornuz, F. Le Formal, N. Tetreault, K. Sivula, and M. Grätzel: A Ga_2O_3 underlayer as an isomorphic template for ultrathin hematite films toward efficient photoelectrochemical water splitting. *Faraday Discuss.* **155**, 223 (2012).
48. F.L. Souza, K.P. Lopes, E. Longo, and E.R. Leite: The influence of the film thickness of nanostructured alpha-Fe_2O_3 on water photooxidation. *Phys. Chem. Chem. Phys.* **11**(8), 1215 (2009).
49. F. Le Formal, M. Grätzel, and K. Sivula: Controlling photoactivity in ultrathin hematite films for solar water-splitting. *Adv. Funct. Mater.* **20**(7), 1099 (2010).
50. O. Zandi, B.M. Klahr, and T.W. Hamann: Highly photoactive Ti-doped α-Fe_2O_3 thin film electrodes: Resurrection of the dead layer. *Energy Environ. Sci.* **6**(2), 634 (2013).
51. U. Bjoerksten, J. Moser, and M. Grätzel: Photoelectrochemical studies on nanocrystalline hematite films. *Chem. Mater.* **6**(6), 858 (1994).
52. B.I. Kharisov, O.V. Kharissova, and M. Jose-Yacaman: Nanostructures with animal-like shapes. *Ind. Eng. Chem. Res.* **49**(18), 8289 (2010).
53. L. Armelao, G. Granozzi, E. Tondello, P. Colombo, G. Principi, P.P. Lottici, and G. Antonioli: Nanocrystalline α-Fe_2O_3 sol-gel thin films: A microstructural study. *J. Non-Cryst. Solids* **192–193**, 435 (1995).
54. K. Woo, H.J. Lee, J.P. Ahn, and Y.S. Park: Sol–gel mediated synthesis of Fe_2O_3 nanorods. *Adv. Mater.* **15**(20), 1761 (2003).
55. A. Mao, G.Y. Han, and J.H. Park: Synthesis and photoelectrochemical cell properties of vertically grown α-Fe_2O_3 nanorod arrays on a gold nanorod substrate. *J. Mater. Chem.* **20**(11), 2247 (2010).
56. S.K. Mohapatra, S.E. John, S. Banerjee, and M. Misra: Water photooxidation by smooth and ultrathin α-Fe_2O_3 nanotube arrays. *Chem. Mater.* **21**(14), 3048 (2009).
57. A.S.N. Murth and K.S. Reddy: Photoelectrochemical behaviour of undoped ferric oxide (α-Fe_2O_3) electrodes prepared by spray pyrolysis. *Mater. Res. Bull.* **19**(2), 241 (1984).
58. A. Duret and M. Grätzel: Visible light-induced water oxidation on mesoscopic alpha-Fe_2O_3 films made by ultrasonic spray pyrolysis. *J. Phys. Chem. B* **109**(36), 17184 (2005).
59. F. Le Formal, K. Sivula, and M. Grätzel: The transient photocurrent and photovoltage behavior of a hematite photoanode under working conditions and the influence of surface treatments. *J. Phys. Chem. C* **116**(51), 26707 (2012).
60. N. Beermann, L. Vayssieres, S-E. Lindquist, and A. Hagfeldt: Photoelectrochemical studies of oriented nanorod thin films of hematite. *J. Electrochem. Soc.* **147**(7), 2456 (2000).
61. D.A. Wheeler, G. Wang, Y. Ling, Y. Li, and J.Z. Zhang: Nanostructured hematite: Synthesis, characterization, charge carrier dynamics, and photoelectrochemical properties. *Energy Environ. Sci.* **5**(5), 6682 (2012).
62. C. Jorand Sartoretti, B.D. Alexander, R. Solarska, I.A. Rutkowska, J. Augustynski, and R. Cerny: Photoelectrochemical oxidation of water at transparent ferric oxide film electrodes. *J. Phys. Chem. B* **109**(28), 13685 (2005).
63. A.B.F. Martinson, M.J. DeVries, J.A. Libera, S.T. Christensen, J.T. Hupp, M.J. Pellin, and J.W. Elam: Atomic layer deposition of Fe_2O_3 using ferrocene and ozone. *J. Phys. Chem. C* **115**(10), 4333 (2011).
64. B.M. Klahr, A.B. Martinson, and T.W. Hamann: Photoelectrochemical investigation of ultrathin film iron oxide solar cells prepared by atomic layer deposition. *Langmuir* **27**(1), 461 (2011).
65. K. Sivula, R. Zboril, F. Le Formal, R. Robert, A. Weidenkaff, J. Tucek, J. Frydrych, and M. Grätzel: Photoelectrochemical water splitting with mesoporous hematite prepared by a solution-based colloidal approach. *J. Am. Chem. Soc.* **132**(21), 7436 (2010).
66. D.K. Zhong, M. Cornuz, K. Sivula, M. Grätzel, and D.R. Gamelin: Photo-assisted electrodeposition of cobalt–phosphate (Co–Pi) catalyst on hematite photoanodes for solar water oxidation. *Energy Environ. Sci.* **4**(5), 1759 (2011).
67. A. Mao, J.K. Kim, K. Shin, D.H. Wang, P.J. Yoo, G.Y. Han, and J.H. Park: Hematite modified tungsten trioxide nanoparticle photoanode for solar water oxidation. *J. Power Sources* **210**, 32 (2012).
68. L-S. Zhong, J-S. Hu, H-P. Liang, A-M. Cao, W-G. Song, and L-J. Wan: Self-assembled 3D flowerlike iron oxide nanostructures and their application in water treatment. *Adv. Mater.* **18**(18), 2426 (2006).
69. H.J. Kim, K.I. Choi, A.Q. Pan, I.D. Kim, H.R. Kim, K.M. Kim, C.W. Na, G.Z. Cao, and J.H. Lee: Template-free solvothermal synthesis of hollow hematite spheres and their applications in gas sensors and Li-ion batteries. *J. Mater. Chem.* **21**(18), 6549 (2011).
70. J. Li, X. Lai, C. Xing, and D. Wang: One-pot synthesis of porous hematite hollow microspheres and their application in water treatment. *J. Nanosci. Nanotechnol.* **10**(11), 7707 (2010).
71. K.S. Lin, Z.P. Wang, S. Chowdhury, and A.K. Adhikari: Preparation and characterization of aligned iron nanorod using aqueous chemical method. *Thin Solid Films* **517**(17), 5192 (2009).
72. D.K. Bora, A. Braun, R. Erni, G. Fortunato, T. Graule, and E.C. Constable: Hydrothermal treatment of a hematite film leads to highly oriented faceted nanostructures with enhanced photocurrents. *Chem. Mater.* **23**(8), 2051 (2011).
73. L. Xi, P.D. Tran, S.Y. Chiam, P.S. Bassi, W.F. Mak, H.K. Mulmudi, S.K. Batabyal, J. Barber, J.S.C. Loo, and L.H. Wong: Co_3O_4-decorated hematite nanorods as an effective photoanode for solar water oxidation. *J. Phys. Chem. C* **116**(26), 13884 (2012).
74. J. Deng, J. Zhong, A. Pu, D. Zhang, M. Li, X. Sun, and S-T. Lee: Ti-doped hematite nanostructures for solar water splitting with high efficiency. *J. Appl. Phys.* **112**, 084312 (2012).
75. S.C. Warren, K. Voïtchovsky, H. Dotan, C.M. Leroy, M. Cornuz, F. Stellacci, C. Hébert, A. Rothschild, and M. Grätzel: Identifying champion nanostructures for solar water-splitting. *Nat. Mater.* **12**, 842 (2013).
76. J-J. Wu, Y-L. Lee, H-H. Chiang, and D.K-P. Wong: Growth and magnetic properties of oriented α-Fe_2O_3 nanorods. *J. Phys. Chem. B* **110**, 18108 (2006).

https://doi.org/10.1557/jmr.2013.302 Published online by Cambridge University Press

77. A. Mao, N-G. Park, G.Y. Han, and J.H. Park: Controlled growth of vertically oriented hematite/Pt composite nanorod arrays: Use for photoelectrochemical water splitting. *Nanotechnology* **22**, 175703 (2011).
78. P.M. Rao and X.L. Zheng: Rapid catalyst-free flame synthesis of dense, aligned α-Fe_2O_3 nanoflake and CuO nanoneedle arrays. *Nano Lett.* **9**, 3001 (2009).
79. A.G. Nasibulin, S. Rackauskas, H. Jiang, Y. Tian, P.R. Mudimela, S.D. Shandakov, L. Nasibulina, J. Sainio, and E.I. Kauppinen: Simple and rapid synthesis of α-Fe_2O_3 nanowires under ambient conditions. *Nano Res.* **2**, 373 (2009).
80. T. Vincent, M. Gross, H. Dotan, and A. Rothschild: Thermally oxidized iron oxide nanoarchitectures for hydrogen production by solar-induced water splitting. *Int. J. Hydrogen Energy* **37**, 8102–8109 (2012).
81. Y. Lin, S. Zhou, S.W. Sheehan, and D. Wang: Nanonet-based hematite heteronanostructures for efficient solar water splitting. *J. Am. Chem. Soc.* **133**, 2398 (2011).
82. V.A.N. de Carvalho, R.A.S. Luz, B.H. Lima, F.N. Crespilho, E.R. Leite, and F.L. Souza: Highly oriented hematite nanorods arrays for photoelectrochemical water splitting. *J. Power Sources* **205**, 525 (2012).
83. L.C. Ferraz, W.M. Carvalho, Jr., D. Criado, and F.L. Souza: Vertically oriented iron oxide films produced by hydrothermal process: Effect of thermal treatment on the physical chemical properties. *ACS Appl. Mater. Interfaces* **4**(10), 5515 (2012).
84. X. Hu and J.C. Yu: Continuous aspect-ratio tuning and fine shape control of monodisperse α-Fe_2O_3 nanocrystals by a programmed microwave–hydrothermal method. *Adv. Funct. Mater.* **18**(6), 880 (2008).
85. L. Vayssieres, A. Hagfeldt, and S.E. Lindquist: Purpose-built metal oxide nanomaterials. The emergence of a new generation of smart materials. *Pure Appl. Chem.* **72**(1–2), 47 (2000).
86. C.X. Kronawitter, I. Zegkinoglou, S. Shen, J. Guo, F.J. Himpsel, S.S. Mao, and L. Vayssieres: On the orbital anisotropy in hematite nanorod-based photoanodes. *Phys. Chem. Chem. Phys.* **15**, 13483 (2013).
87. S. Shen, P. Guo, D.A. Wheeler, J. Jiang, S.A. Lindley, C.X. Kronawitter, J.Z. Zhang, L. Guo, and S.S. Mao: Physical and photoelectrochemical properties of Zr-doped hematite nanorod arrays. *Nanoscale*, 9867–9874 (2013).
88. C.X. Kronawitter, L. Vayssieres, S. Shen, L. Guo, D.A. Wheeler, J.Z. Zhang, B.R. Antoun, and S.S. Mao: A perspective on solar-driven water splitting with all-oxide hetero-nanostructures. *Energy Environ. Sci.* **4**, 3889 (2011).
89. K. Byrappa and M. Yoshimura: Hydrothermal technology: Principles and applications. In *Handbook of Hydrothermal Technology* (William Andrew Publishing, Norwich, NY, 2001); p. 1.
90. G. Morey and P. Niggli: The hydrothermal formation of silicates: A review. *J. Am. Chem. Soc.* **35**(9), 1086 (1913).
91. M.M. Lencka, A. Anderko, and R.E. Riman: Hydrothermal precipitation of lead zirconate titanate solid solutions: Thermodynamic modeling and experimental synthesis. *J. Am. Ceram. Soc.* **78**(10), 2609 (1995).
92. J.O. Eckert, C.C. Hung-Houston, B.L. Gersten, M.M. Lencka, and R.E. Riman: Kinetics and mechanisms of hydrothermal synthesis of barium titanate. *J. Am. Ceram. Soc.* **79**(11), 2929 (1996).
93. A.N. Christensen, M-L. Savolainen, G. Johansson, O. Tolboe, and J. Paasivirta: Hydrothermal preparation of goethite and hematite from amorphous iron(III) hydroxide. *Acta Chem. Scand.* **22**, 1487 (1968).
94. M.A. Blesa and E. Matijević: Phase-transformations of iron-oxides, oxohydroxides, and hydrous oxides in aqueous-media. *Adv. Colloid Interface Sci.* **29**(3–4), 173 (1989).
95. L. Vayssieres: On the design of advanced metal oxide nanomaterials. *Int. J. Nanotechnol.* **1**(1–2), 1 (2004).
96. L. Vayssieres, N. Beermann, S-E. Lindquist, and A. Hagfeldt: Controlled aqueous chemical growth of oriented three-dimensional crystalline nanorod arrays: Application to iron(III) oxides. *Chem. Mater.* **13**(2), 233 (2001).
97. P. Wang, D. Wang, J. Lin, X. Li, C. Peng, X. Gao, Q. Huang, J. Wang, H. Xu, and C. Fan: Lattice defect-enhanced hydrogen production in nanostructured hematite-based photoelectrochemical device. *ACS Appl. Mater. Interfaces* **4**(4), 2295 (2012).
98. S. Shen, C.X. Kronawitter, J. Jiang, S.S. Mao, and L. Guo: Surface tuning for promoted charge transfer in hematite nanorod arrays as water-splitting photoanodes. *Nano Res.* **5**(5), 327 (2012).
99. T. Lindgren, H.L. Wang, N. Beermann, L. Vayssieres, A. Hagfeldt, and S.E. Lindquist: Aqueous photoelectrochemistry of hematite nanorod array. *Sol. Energy Mater. Sol. Cells* **71**(2), 231 (2002).
100. L. Vayssieres, C. Sathe, S.M. Butorin, D.K. Shuh, J. Nordgren, and J. Guo: One-dimensional quantum-confinement effect in α-Fe_2O_3 ultrafine nanorod arrays. *Adv. Mater.* **17**(19), 2320 (2005).
101. R. Morrish, M. Rahman, J.M. MacElroy, and C.A. Wolden: Activation of hematite nanorod arrays for photoelectrochemical water splitting. *ChemSusChem* **4**(4), 474 (2011).
102. J.S. Jang, J. Lee, H. Ye, F-R.F. Fan, and A.J. Bard: Rapid screening of effective dopants for Fe_2O_3 photocatalysts with scanning electrochemical microscopy and investigation of their photoelectrochemical properties. *J. Phys. Chem. C* **113**(16), 6719 (2009).
103. P. Kumar, P. Sharma, R. Shrivastav, S. Dass, and V.R. Satsangi: Electrodeposited zirconium-doped α-Fe_2O_3 thin film for photoelectrochemical water splitting. *Int. J. Hydrogen Energy* **36**(4), 2777 (2011).
104. Y-S. Hu, A. Kleiman-Shwarsctein, A.J. Forman, D. Hazen, J-N. Park, and E.W. McFarland: Pt-doped α-Fe_2O_3 thin films active for photoelectrochemical water splitting. *Chem. Mater.* **20**(12), 3803 (2008).
105. K. Sivula: Metal oxide photoelectrodes for solar fuel production, surface traps, and catalysis. *J. Phys. Chem. Lett.* **4**(10), 1624–1633 (2013).
106. Y. Ling, G. Wang, J. Reddy, C. Wang, J.Z. Zhang, and Y. Li: The influence of oxygen content on the thermal activation of hematite nanowires. *Angew. Chem. Int. Ed.* **51**(17), 4074 (2012).
107. M.W. Kanan and D.G. Nocera: In situ formation of an oxygen-evolving catalyst in neutral water containing phosphate and Co^{2+}. *Science* **321**(5892), 1072 (2008).
108. L. Kavan, K. Kratochvilova, and M. Grätzel: Study of nanocrystalline TiO_2 (anatase) electrode in the accumulation regime. *J. Electroanal. Chem.* **394**(1–2), 93 (1995).
109. R.C. Stehle, M.M. Bobek, R. Hooper, and D.W. Hahn: Oxidation reaction kinetics for the steam-iron process in support of hydrogen production. *Int. J. Hydrogen Energy* **36**(23), 15125 (2011).
110. J. Bisquert, F. Fabregat-Santiago, I. Mora-Seró, G. Garcia-Belmonte, E.M. Barea, and E. Palomares: A review of recent results on electrochemical determination of the density of electronic states of nanostructured metal-oxide semiconductors and organic hole conductors. *Inorg. Chim. Acta* **361**(3), 684 (2008).
111. J.W. Schultze: Electrochemistry of novel materials. *Adv. Mater.* **8**(4), 360 (1994).
112. A.M. Xavier, F.F. Ferreira, and F.L. Souza: Morphological and structural evolution of one dimensional hematite nanorods. *RSC Adv.* (2013, accepted).
113. T.R. Cook, D.K. Dogutan, S.Y. Reece, Y. Surendranath, T.S. Teets, and D.G. Nocera: Solar energy supply and storage for the legacy and nonlegacy worlds. *Chem. Rev.* **110**(11), 6474 (2010).
114. D.K. Zhong and D.R. Gamelin: Photoelectrochemical water oxidation by cobalt catalyst ("Co-Pi")/alpha-Fe_2O_3 composite

https://doi.org/10.1557/jmr.2013.302 Published online by Cambridge University Press

photoanodes: Oxygen evolution and resolution of a kinetic bottleneck. *J. Am. Chem. Soc.* **132**(12), 4202 (2010).
115. D.R. Gamelin: Water splitting: Catalyst or spectator? *Nat. Chem.* **4**(12), 965 (2012).
116. V. Aroutiounian: Investigation of ceramic $Fe_2O_3\langle T_a\rangle$ photoelectrodes for solar energy photoelectrochemical converters. *Int. J. Hydrogen Energy* **27**(1), 33 (2002).
117. J.S. Jang, K.Y. Yoon, X. Xiao, F-R.F. Fan, and A.J. Bard: Development of a potential Fe_2O_3-based photocatalyst thin film for water oxidation by scanning electrochemical microscopy: Effects of Ag−Fe_2O_3 nanocomposite and Sn doping. *Chem. Mater.* **21**(20), 4803 (2009).
118. K.J. McDonald and K-S. Choi: Photodeposition of co-based oxygen evolution catalysts on α-Fe_2O_3 photoanodes. *Chem. Mater.* **23**(7), 1686 (2011).
119. D.K. Zhong, J. Sun, H. Inumaru, and D.R. Gamelin: Solar water oxidation by composite catalyst/alpha-Fe_2O_3 photoanodes. *J. Am. Chem. Soc.* **131**(17), 6086 (2009).
120. Y.R. Hong, Z. Liu, S.F. Al-Bukhari, C.J. Lee, D.L. Yung, D. Chi, and T.S. Hor: Effect of oxygen evolution catalysts on hematite nanorods for solar water oxidation. *Chem. Commun.* **47**(38), 10653 (2011).
121. H.G. Cha, J. Song, H.S. Kim, W. Shin, K.B. Yoon, and Y.S. Kang: Facile preparation of Fe_2O_3 thin film with photoelectrochemical properties. *Chem. Commun.* **47**(8), 2441 (2011).
122. Y. Hou, F. Zuo, A. Dagg, and P. Feng: Visible light-driven alpha-Fe_2O_3 nanorod/graphene/$BiV_{1-x}Mo_xO_4$ core/shell heterojunction array for efficient photoelectrochemical water splitting. *Nano Lett.* **12**(12), 6464 (2012).
123. L. Xi, S.Y. Chiam, W.F. Mak, P.D. Tran, J. Barber, S.C.J. Loo, and L.H. Wong: A novel strategy for surface treatment on hematite photoanode for efficient water oxidation. *Chem. Sci.* **4**(1), 164 (2013).
124. R.L. Spray, K.J. McDonald, and K-S. Choi: Enhancing photoresponse of nanoparticulate α-Fe_2O_3 electrodes by surface composition tuning. *J. Phys. Chem. C* **115**(8), 3497 (2011).
125. K.J. McDonald and K-S. Choi: Synthesis and photoelectrochemical properties of $Fe_2O_3/ZnFe_2O_4$ composite photoanodes for use in solar water oxidation. *Chem. Mater.* **23**(21), 4863 (2011).
126. H. Dotan, K. Sivula, M. Grätzel, A. Rothschild, and S.C. Warren: Probing the photoelectrochemical properties of hematite (α-Fe_2O_3) electrodes using hydrogen peroxide as a hole scavenger. *Energy Environ. Sci.* **4**, 958 (2011).
127. B.M. Klahr and T.W. Hamann: Current and voltage limiting processes in thin film hematite electrodes. *J. Phys. Chem. C* **115**(16), 8393 (2011).
128. G. Rahman and O-S. Joo: Photoelectrochemical water splitting at nanostructured α-Fe_2O_3 electrodes. *Int. J. Hydrogen Energy* **37**(19), 13989 (2012).

https://doi.org/10.1557/jmr.2013.302 Published online by Cambridge University Press